

Intratumoral delivery of a Tim-3 antibody-encoding oncolytic adenovirus engages an effective antitumor immune response in liver cancer

qiang li

Zhejiang Sci-Tech University

hui Zhang

Zhejiang Sci-Tech University

leilei Zhang

Zhejiang Sci-Tech University

Xiaoyan Wang

Oncology Department, Zhejiang Xiaoshan hospital

hui wang

Oncology Department, Zhejiang Xiaoshan hospital

Biao Huang

Zhejiang Sci-Tech University

Yigang Wang (✉ ygwang@zstu.edu.cn)

Zhejiang Sci-Tech University

Fang Huang

Department of Pathology, Zhejiang Provincial People's Hospital

Yiqiang Wang

Surgical Department of Duchang County Second People's Hospital

Research Article

Keywords: hepatocellular carcinoma, Oncolytic adenovirus, α -TIM-3, immunoreactivity

Posted Date: August 11th, 2023

DOI: <https://doi.org/10.21203/rs.3.rs-3239891/v1>

License:   This work is licensed under a Creative Commons Attribution 4.0 International License.

[Read Full License](#)

Additional Declarations: No competing interests reported.

Version of Record: A version of this preprint was published at Journal of Cancer Research and Clinical Oncology on December 11th, 2023. See the published version at <https://doi.org/10.1007/s00432-023-05501-8>.

Abstract

The use of oncolytic viruses as a gene therapy vector is an area of active biomedical research, particularly in the context of cancer treatment. However, the actual therapeutic success of this approach to tumor elimination remains limited. As such, the present study was developed with the goal of simultaneously enhancing the antitumor efficacy of oncolytic viruses and the local immune response by combining the Ad-GD55 oncolytic adenovirus and an antibody specific for the TIM-3 immune checkpoint molecule (α -TIM-3). The resultant Ad-GD55- α -Tim-3 oncolytic adenovirus is capable of inducing α -TIM-3 expression within hepatoma cells upon infection, and Ad-GD55- α -Tim-3 exhibited inhibitory efficacy superior to that of Ad-GD55 when used to treat these tumor cells together with the induction of enhanced intracellular immunity. In vivo experiments revealed that Ad-GD55- α -TIM-3 administration was sufficient to inhibit tumor growth and to engage a more robust local immune response within the simulated tumor immune microenvironment. As such, this Ad-GD55- α -TIM-3 oncolytic adenovirus may represent a viable approach to the treatment of hepatocellular carcinoma.

1 Introduction

In 2020, statistics released by the World Health Organization estimate that primary liver tumors are the 6th most prevalent tumor type among 36 cancers, in addition to being the 3rd deadliest form of cancer with an estimated 906,000 diagnoses and 830,000 deaths (Sung et al., 2021; Tseng et al., 2020). Liver tumors develop, invade local tissues, and metastasize over extended periods of time through multifactorial and complex ongoing processes (Tang et al., 2022). Major drivers of hepatocellular carcinoma (HCC) incidence include high body weight, type 2 diabetes, smoking, excessive drinking, and certain chronic infections (Czauderna et al., 2019; Thongsri et al., 2021; Villanueva, 2019). The number of patients with tumors induced as a result of these risk factors is rising annually, particularly in nations with higher standards of living. The primary approach to treating HCC consists of surgical tumor resection and chemoradiotherapy. The FDA has approved multiple drugs including Sorafenib, Regorafenib, and Lenvatinib as treatment options for individuals with advanced HCC, but response rates remain suboptimal and patient prognostic outcomes remain poor (Cao et al., 2020; Chen et al., 2019; Jia et al., 2022). As such, there is a pressing need for efforts to identify novel approaches to managing and treating liver cancer that can yield greater therapeutic efficacy.

Recent efforts have highlighted the promise of oncolytic viruses owing to their ability to infect and lyse tumor cells with a high degree of specificity, minimizing their effects on healthy cells. These viral particles can infect tumor cells through indirect or direct mechanisms and may express cytotoxic proteins or drive the induction of antitumor immunity following the expression of important tumor epitopes (Chen et al., 2021; Chen et al., 2022a; Chen et al., 2022b). Genetic engineering and the use of tumor-specific promoters can further enhance the ability of oncolytic viruses to replicate specifically within tumors (Lin et al., 2018; Raja et al., 2018; Yoshida et al., 2021). In a prior report, we developed the liver cancer-specific Ad-GD55 oncolytic adenovirus that expresses E1A, which is essential for ZD55 viral replication, under the control of the tumor-targeted GP73 promoter (Ying et al., 2018). Oncolytic viruses can effectively promote both

innate and adaptive antitumor immunity(Das et al., 2021), and the success of immunotherapeutic interventions and the resultant immune response is dependent upon interactions among cells and signaling molecules that include chemokines and cytokines (Ishino et al., 2021). Studies of the mechanisms that govern oncolytic viral infections and the consequent changes in the composition of the tumor immune microenvironment (TIME) highlight the promise of this therapeutic approach, transforming immunologically inert 'cold' tumors into active 'hot' tumors through synergistic effects with immune checkpoint inhibitors (ICIs) targeting PD-1, CTLA4, and PD-L1(LaRocca and Warner, 2018; Wang et al., 2020).

The immunosuppressive TIM-3 (T-cell immunoglobulin domain and mucin-domain molecule-3) protein is an immune checkpoint and target of second-generation ICIs(Sabatos-Peyton et al., 2018). The initial discovery of TIM-3 expression on the surface of differentiated Th1 cells revealed that it functions as a regulator of macrophage activation capable of influencing the severity of autoimmune encephalomyelitis(Monney et al., 2002). Administering anti-TIM-3 antibodies to patients with cancer can provoke more robust tumor antigen expression and cytokine release(Qin et al., 2020). Tumor-infiltrating lymphocytes express both PD-1 and TIM-3, and combined therapeutic blocking antibody regimens targeting these two molecules have achieved superior antitumor efficacy in preclinical research(Zhu et al., 2015). TIM-3 expression has also been reported on other cells including NK cells, dendritic cells, and ovarian, renal, and liver cancer cells(Xiao et al., 2020). Functionally, TIM-3 is closely tied to liver cancer development given its ability to mediate T cell dysfunction, contributing to worse patient outcomes. Polymorphisms in the TIM-3 gene are also linked to HCC and cirrhosis incidence in hepatitis patients(Li et al., 2012). Tumor-associated macrophages and liver tumor tissue samples reportedly express higher TIM-3 levels than healthy liver tissue(Li et al., 2016). These data suggest that TIM-3 may function as a key regulator of liver cancer incidence and resistance to treatment, highlighting new potential avenues for immunotherapeutic intervention.

For the present analysis, the combined effects of the oncolytic Ad-GD55 virus and TIM-3 blockade on liver cancer were assessed by generating a novel recombinant Ad-GD55- α -TIM-3 oncolytic virus encoding the full-length TIM-3 antibody gene. This Ad-GD55- α -TIM-3 virus is capable of specifically replicating within HCC cells and facilitating the expression of α -TIM-3. Ad-GD55- α -TIM-3 treatment can suppress the proliferation of HCC cells and promote cytokine secretion, while also significantly inhibiting tumor growth and enhancing antitumor immune response induction in a xenograft mouse model system. Together, these data suggest that oncolytic viruses can be combined with TIM-3 inhibition when treating liver cancer, emphasizing the clinical potential of this novel Ad-GD55- α -TIM-3 vector.

2 Materials and methods

Cell culture

Human BEL-7404, MHCC-97H, SMMC-7721, and Huh7 HCC cells and control human WRL-68 cells from the Type Culture Collection of the Chinese Academy of Sciences (Shanghai, China) were cultured in

DMEM containing 10% heat-inactivated fetal bovine serum (FBS, Gibco) in a 37°C, 5% CO₂ incubator.

Oncolytic virus preparation

The oncolytic Ad-GD55- α -TIM-3 virus was prepared by inserting the coding sequence for full-length anti-TIM-3 into the previously constructed liver-specific Ad-GD55 oncolytic adenoviral vector (Ying et al., 2018). Recombinant Ad-GD55- α -TIM-3 and Ad-GD55 amplification was performed using 293A cells, with cesium chloride gradient ultracentrifugation for purification. TCID₅₀ (median tissue culture infectious dose) assays were used to calculate the viral titer.

Viral progeny assay

WRL-68, BEL-7404, and MHCC-97H were plated in 24-well plates (4×10^4 /well) followed by infection at a multiplicity of infection (MOI) of 10 with Ad-GD55 or Ad-GD55- α -TIM-3. At 6 h post-infection, media was removed and cells were rinsed twice using PBS, followed by the addition of fresh media. Following a further 48 h incubation, cells and media were harvested, and virus-containing supernatants were collected via three rounds of freeze-thawing and centrifugation. TCID₅₀ assays were used to measure viral titers in HEK293 cells based on a standard approach.

Cell viability assay

Following plating overnight in 96-well plates (5,000/well), cells were infected with Ad-GD55 or Ad-GD55- α -TIM-3 (MOI = 10). Following infection for 24, 48, 72, or 96 h, MTT reagent (0.5 mg/ml, 20 μ L/well) was added to each well for 4 h. After removing media from each well, 150 μ L of DMSO was added per well to facilitate formazan dye dissolution. Samples were mixed thoroughly, and a microplate reader was used to quantify absorbance at 490 nm in each well.

Cytopathic assay

BEL-7404, MHCC-97H, SMMC-7721, Huh7, and WRL-68 cells were plated in 24-well plates and cultured until ~ 50% confluent, at which time they were infected with Ad-GD55 or Ad-GD55- α -TIM-3 at a range of MOIs (0, 1, 5, 10, 20, 40 MOIs). Following incubation at 37°C for 96 h, media was removed from all cells followed by staining for 30 min using crystal violet solution (0.1% crystal violet, 20% methanol in water). After rinsing the plates with tap water, they were oven-dried overnight and photographed.

qPCR

TRIZol (Generay, GK3016) was used to harvest RNA from samples, after which a qPCR RT Kit (Takara, 639504) was used for cDNA preparation, and qPCR analyses were performed with SYBR Green Universal TaqMan multiplex qPCR master mix (Yeasen, 11202ES08). GAPDH served as a normalization control. An ABI 7500 qPCR system was used for all qPCR analyses.

Western immunoblotting

Cells were plated overnight in 6-well plates (5×10^5 /well) and infected with Ad-Gd55 or Ad-GD55- α -TIM-3 (MOI = 10). After a 48 h incubation, cells were harvested and lysed in SDS Lysis Buffer (Beyotime, Shanghai, China, P0013G) supplemented with protease inhibitors. Protein levels in the resultant lysates were measured with a BCA assay (Thermo Fisher Scientific, 23225). Then, 20–50 μ g of protein per sample was boiled in SDS loading buffer, separated via 4–15% SDS-PAGE, and transferred onto PVDF membranes that were subsequently blocked for 4 h at room temperature using 5% non-fat milk (Yeasen, 36120ES76). Primary antibodies specific for GAPDH (Santa Cruz, sc-365062), BAX (Santa Cruz, sc-7480), Bcl-2 (Santa Cruz, sc-7382), TIM-3 (Huabio, EM1701-20), IL-6 (Santa Cruz, sc-28343), IL-7 (Santa Cruz, sc-365306), TNF- α (Santa Cruz, sc-133192), IL-1 β (Santa Cruz, sc-52012), CAR (Abcam, ab100811), GP73 (Santa Cruz, sc-365817), E1A (Santa Cruz, sc-58658), and His (Abclone, AE003) were then incubated with samples overnight at 4°C. Blots were then probed with appropriate secondary mouse or rabbit antibodies (Huabio, HA1006 or HA1001) at a 1:20,000 dilution for 90 min at room temperature. A fully automatic chemiluminescence image analysis system (Tanon 5200) was then used to detect proteins.

Tumor xenograft model

The Laboratory animal welfare ethics committee of Zhejiang Sci-Tech University approved all animal studies (Protocol number: 202110001, date of approval: 5th October 2021). Blood samples were obtained from healthy volunteers. Peripheral blood mononuclear cells (PBMCs) were isolated from Ficoll (Solarbio) by density-gradient centrifugation. Briefly, fresh PBMCs were activated on day - 20 using 6-well plates coated with 3 mg/mL anti-CD3 antibody (BD pharmingen, Cat# 555329) and 1 mg/mL anti-CD28 antibody (BD pharmingen, Cat# 555725) followed by culture in RPMI-1640 supplemented with 10% FBS, 100 U/mL IL-2 (Sino biological, Cat#11848-HNAE2), 2 mM GlutaMAX (Thermo Fisher, Cat# 35050061), and penicillin/streptomycin (GIBCO, Cat# 15140-122). BEL-7404 cells were plated in 6-well plates on day - 17 (5×10^5 /well) and, following a 6 h incubation, these cells were treated for 2 h with mitomycin C (10 mg/mL) for 2 h followed by two washed with PBS. The resultant cells were then combined with activated PBMCs (5×10^6) for co-culture at a 10:1 PBMC: BEL-7404 ratio. Every other day, PBMCs were harvested and repeatedly cultured with mitomycin C-treated BEL-7404 cells using this same approach. After 3 rounds of co-culture, PBMCs were collected and combined with fresh BEL-7404 cells at a 1:4 ratio (BEL-7404 = 1×10^7 , PBMC = 2.5×10^6) (Li et al., 2020). The resultant mixed cell preparation was injected into the flank of BALB/c nude mice (females, 6–8 weeks old). When tumors were $\sim 100 \text{ mm}^3$ in size, two total intratumoral injections of PBS, Ad-GD55 (1×10^9 PFU/100 μ L), or Ad-GD55- α -TIM-3 (1×10^9 PFU/100 μ L) were administered at an interval of 2 days. Tumor volume measurements were taken every 5 days as follows: volume = (length \times width²)/2. After 30 days, mice were euthanized and samples of liver, spleen, kidney, and tumor tissues were harvested for analysis.

Histological and immunohistochemical staining

Harvested samples of renal, hepatic, splenic, and tumor tissues were fixed using 4% paraformaldehyde, dehydrated with 70% ethanol, and embedded in paraffin. For morphological analyses, tissue sections were stained using hematoxylin and eosin (H&E). For immunohistochemical (IHC) staining, tumor

sections were probed with monoclonal mouse antibodies specific for human CD4, CD8, Ki-67, and adenoviral hexon. After rinsing with PBS, these sections were probed with HRP-conjugated goat anti-mouse IgG, rinsed with PBS, incubated with avidin-biotin-peroxidase (Vector Laboratories, CA, USA), and developed using DAB.

ELISAs

Harvested tissue samples were homogenized 10 times with a homogenizer, lysed in SDS cell lysis solution, centrifuged (12,000 rpm, 10 min, 4°C), and supernatants were harvested for downstream analysis. Human TNF- α (Sino biological, CAT#KIT10602) and Human IFN- γ (Sino biological, CAT#KIT11725A) ELISA kits were then used based on provided directions. Briefly, after warming reagents to room temperature for a minimum of 30 min, 96-well plates were coated with recombinant antigen overnight at 4°C, washed, blocked with blocking buffer, and serial 10-fold dilutions of each tissue lysate sample (prepared in PBS) were added per well for 2 h at room temperature. A diluted HRP-conjugated detection antibody was then added for 1 h at room temperature, followed by the addition of the prepared substrate solution. The color development reaction was terminated by adding Stop Solution at an appropriate time point, and a microplate reader was used to quantify absorbance at 450 nm.

Statistical analysis

GraphPad Prism 7 (GraphPad Software, CA, USA) was used to analyze data. *In vitro* results were analyzed in triplicate while animal studies were performed one time. Results were compared with unpaired t-tests. *P < 0.05, **P < 0.01, ***P < 0.001, ****P < 0.0001, NS: not significant. Data are given as means with standard deviations.

3 Results

Characterization of TIM-3 expression in liver tumors and healthy liver tissue

High TIM-3 expression has previously been reported in liver cancer tissues and cells from humans. Consistently, the present analyses revealed significantly elevated TIM-3 expression in three liver cancer tissue samples relative to paracancerous tissues (Fig. 1A). TIM-3 protein levels were also upregulated in all analyzed HCC cell lines other than SMMC-7721 cells in comparison with control WRL-68 cells (Fig. 1B), and the same was true at the mRNA level (Fig. 1C). TIM-3 thus represents a promising therapeutic target for novel approaches to treating liver cancer.

The success of oncolytic virus therapy is also dependent on the selection of an appropriate and selective tumor target. Previously, our team determined that GP73 is an ideal liver cancer-specific target, with the GP73-regulated GD55 oncolytic virus exerting good antitumor efficacy in a xenograft model of liver cancer. GP73 and Coxsackievirus and Adenovirus Receptor (CAR) expression levels were therefore analyzed in HCC and normal hepatic cells, revealing higher levels of GP73 expression in all HCC cells

other than SMMC-7721 cells when compared to control WRL-68 cells, whereas CAR expression was detectable across all cells (Fig. 1B and Supplemental Fig. 1).

Ad-GD55- α -TIM-3 oncolytic adenovirus preparation and characterization

Given the promising performance of the oncolytic GC55 virus, the novel Ad-GD55- α -TIM-3 virus was herein constructed in which viral replication is under the control of the GP73 promoter and the virus encodes a full-length anti-TIM-3 antibody gene. In this virus, the Ad5 E1A promoter was substituted for the GP73 promoter and the α -TIM-3 gene was inserted into the region of the deleted 55 kDa E1B gene (Fig. 2A). α -TIM-3 and adenoviral E1A expression levels were then analyzed in infected BEL-7404 HCC cells, revealing that E1A expression was strongly induced by both Ad-GD55 and Ad-GD55- α -TIM-3, whereas only Ad-GD55- α -TIM-3 induced the expression of α -TIM-3 antibodies in virally infected cells (Fig. 2B). To test the effects of inserting the α -TIM-3 gene into these viruses, the ability of the Ad-GD55- α -TIM-3 viral progeny to replicate were analyzed, revealing no differences in progeny virus recovery when comparing HCC cells infected with Ad-GD55 or Ad-GD55- α -TIM-3. Significantly higher progeny virus numbers were observed in virally infected tumor cells relative to control WRL-68 cells following viral infection (Fig. 2C). These data suggest that Ad-GD55- α -TIM-3 can undergo specific replication in HCC cells, thereby inducing α -TIM-3 expression.

Ad-GD55- α -TIM-3 induces tumor-specific cytotoxic activity in HCC cells

An MTT assay was next used to assess the viability of HCC cells (BEL-7404, Huh7, or MHCC-97H) and control WRL-68 cells infected at an MOI of 10 with the indicated viruses. Time-dependent cytotoxic cell death was evident following the infection of HCC cells with the Ad-GD55- α -TIM-3 virus, and the cytotoxic effects of Ad-GD55- α -TIM-3 were superior to those of Ad-GD55 without any clear cytotoxic effects in WRL-68 cells infected with either of these viruses. Crystal violet staining was used to quantify the cytopathic effect, confirming that Ad-GD55- α -TIM-3 induced a stronger cytopathic effect than Ad-GD55 in HCC cells in a dose-dependent manner without adversely impacting WRL-68 cells (Fig. 3B). This oncolytic Ad-GD55- α -TIM-3 virus can thus induce tumor cell death in a specific manner while minimally impacting healthy cells, offering an effective tumor targeting strategy.

Investigation of the mechanisms through which Ad-GD55- α -TIM-3 selectively induces antitumor immunity

To better understand the potential mechanisms whereby Ad-GD55- α -TIM-3 modulates inflammatory and immune responses following the infection of HCC cells, a series of qPCR and Western immunoblotting assays were performed in BEL-7404 cells following viral infection for 48 h. Following Ad-GD55 infection, upregulation of the co-inhibitory molecule TIM-3 and its ligands galectin-9 and CEACAM-1 was observed, together with significant increases in the expression of the immune checkpoint ligand ICOSL. In addition, OX40L expression levels were reduced, while Ad-GD55- α -TIM-3 infection reversed this reduction in expression levels. The infection of HCC cells with these oncolytic viruses can thus modulate both co-stimulatory and co-inhibitory ligand expression. Infection with these oncolytic viruses reduced levels of pro-inflammatory IL-1 β and IL-6 while upregulating anti-inflammatory IL-10 (Fig. 4B), and these effects

were more pronounced following Ad-GD55- α -TIM-3 infection relative to Ad-GD55 infection. This suggests that Ad-GD55- α -TIM-3 can suppress local inflammation and generate an environment favorable for viral replication and proliferation. Their Ad-GD55- α -TIM-3 infection of these HCC cells also promoted the upregulation of the immunostimulatory cytokines IL-7, TNF- α , and IL-23 as well as the chemokine CCL19, whereas this effect was not apparent for the control Ad-GD55 virus (Fig. 4C). Relative to control treatment, oncolytic virus infection significantly decreased the expression of immunosuppressive TGF- β and IDO, with comparable efficacy for both Ad-GD55- α -Tim-3 and Ad-GD55 (Fig. 4C). These oncolytic viruses may thus activate the immune response, with the targeted Ad-GD55- α -Tim-3 virus exhibiting a more robust activating effect than the control Ad-GD55.

Changes in cytokine and apoptosis-related protein levels were also analyzed in these infected HCC cells. In line with the above data, IL-6 and IL-1 β expression was reduced by viral infection whereas TNF- α , IL-7, and TIM-3 expression was enhanced (Fig. 4D), with this effect being more robust following Ad-GD55- α -Tim-3 infection. Oncolytic virus infection also resulted in Bax downregulation and Bcl-2 upregulation in these BEL-7404 cells (Fig. 4E), suggesting that Ad-GD55 and Ad-GD55- α -Tim-3 infection did not induce apoptotic cell death. No difference in apoptotic induction was evident when comparing cells infected with these two viruses. Ad-GD55- α -Tim-3 infection also markedly reduced growth-promoting p38 and c-Myc expression as compared to that observed following Ad-GD55 expression (Fig. 4E), suggesting that α -TIM-3 strongly inhibits the growth of HCC cells.

Analysis of the *in vivo* antitumor efficacy of Ad-GD55- α -TIM-3

Given the promising *in vitro* data shown above, the antitumor efficacy of the developed oncolytic Ad-GD55- α -TIM-3 virus was next assessed in a murine xenograft model of HCC. A PBMC co-culture system was used to establish BEL-7404 tumor-bearing mice, thereby providing a means of better mimicking the local tumor microenvironment in a manner more consistent with that in HCC patients (Fig. 5A). Tumor volume was monitored over time in different treatment groups, revealing that intratumoral Ad-GD55- α -TIM-3 injection significantly suppressed tumor growth such that the tumor volume on day 30 was just 683 mm³ as compared to 1035 mm³ and 1509 mm³ in the Ad-GD55 and PBS treatment groups (Fig. 5B). These results thus confirmed the ability of Ad-GD55- α -TIM-3 to significantly suppress the growth of human xenograft tumors.

On day 30, mice were euthanized and tumor sections were subjected to H&E staining that revealed more extensive tumor cell death in the Ad-GD55- α -TIM-3 treatment group relative to the Ad-GD55 or PBS control groups. No mice exhibited evidence of cytopathic changes in the liver, spleen, or kidneys, indicating that these viruses do not induce significant normal tissue toxicity. Ectopic adenoviral hexon protein expression was evident in tumor tissues from oncolytic virus-infected groups as detected via IHC staining, whereas the same was not evident in the PBS control group (Fig. 5C). Lower levels of the proliferation-related Ki-67 antigen expression were evident in the Ad-GD55- α -TIM-3 group relative to the Ad-GD55 or PBS control groups, highlighting the ability of this virus to better suppress tumor growth. When analyzing immune-related protein expression, Ad-GD55- α -TIM-3 was found to induce the intratumoral upregulation of the T

cell marker proteins CD4 and CD8 to a greater degree than was evident in the Ad-GD55 or PBS control groups (Fig. 5D). This suggests that this novel oncolytic virus is capable of modulating the TIME to provoke robust antitumor immunity.

4 Discussion

The development and progression of liver cancer is a multi-step process that is highly complex (Cox et al., 2016). While a range of targeted drugs have been developed that seek to treat HCC by interfering with these pathways and demonstrated a high degree of efficacy in preclinical research or the clinic, many of these agents are less effective in more advanced tumors. Sorafenib, for example, is the first drug to have received approval for the specific treatment of HCC yet it exhibits unsatisfactory efficacy in most clinical applications (Tang et al., 2020). There thus remains a pressing need to design new approaches to treating HCC such as the establishment of more robust oncolytic virotherapy and immunotherapy strategies (Huang et al., 2019; Samson et al., 2022).

Since the initial CDE approval of H101 as an oncolytic viral drug product in 2005, this oncolytic virotherapy strategy has achieved excellent efficacy. Globally, four oncolytic viruses have received approval to date (H101, T-Vec, Rigvir, and Delytact), and several more are undergoing evaluation in clinical trials. Our group proposed the Cancer Targeting Gene-Virotherapy (CTGVT) strategy in 2001 and has made substantial progress in developing oncolytic viruses that have been deployed *in vitro* and *in vivo* in a range of therapeutic trials (Zhang et al., 2003). The emergence of CAR-T therapies and ICI have heralded a new era of advanced immunotherapeutic drug design (Kim et al., 2020). Over 10 ICIs have been designed throughout the world, and first-generation ICIs targeting PD-1 (pembrolizumab) and CTLA-4 (ipilimumab) have achieved success in the treatment of solid tumors (Lebbé et al., 2019; Yi et al., 2018). ICI clinical response rates, however, generally do not exceed 35–40% (Yang et al., 2014). Given that the therapeutic benefits of ICIs or oncolytic viruses in isolation remain limited, clinical trials have increasingly explored their use in combination with promising results (Hwang et al., 2020). Oncolytic viruses are safe and can transform an immunologically 'cold' tumor into an active 'hot' tumor by eliciting immune responses mediated by infiltrating T cells (Ju et al., 2022). The combination of T-Vec and ipilimumab or/and pembrolizumab can reportedly enhance antitumor immunity via the promotion of improved intratumoral T cell infiltration and IFN- γ upregulation while maintaining a good safety profile (Chesney et al., 2018; Ribas et al., 2017). Efforts to combine ICIs with oncolytic viruses can thus effectively treat certain cancers.

TIM-3 is an immune checkpoint receptor expressed by a wide range of immune cell types, making it an ideal target for the induction of more robust antitumor immune responses. Over 5 monoclonal antibodies specific for TIM-3 have been described and deployed in clinical trials or preclinical studies (Bailly et al., 2023). Preliminary work from our group and others revealed that in addition to being highly expressed by T cells and other immune populations, liver cancer cells also exhibit pronounced TIM-3 upregulation (Fig. 1A,B), making it a promising target when treating liver cancer. As such, an engineered Ad-GD55- α -TIM-3 oncolytic virus encoding a TIM-3-specific antibody was herein developed. This virus exhibited

potent antitumor efficacy when used to treat HCC *in vitro* and *in vivo* with minimal adverse effects on normal cells (Fig. 3A,B). This oncolytic virus strongly inhibited liver tumor cell growth and suppressed the expression of c-Myc, which is associated with malignant growth and poor prognostic outcomes (Fig. 4E). This oncolytic virus was also able to impact immune- and inflammation-related factor production by liver cancer cells, enhancing antitumor immunity via the reshaping of the TIME (Fig. 4D). These results align well with findings from prior reports (Lang et al., 2018; Minott et al., 2022). The antitumor immune efficacy of AD-GD55- α -TIM-3 was superior to that of the Ad-GD55 control virus, consistent with the beneficial and potent effects of α -TIM-3 expression.

Oncolytic virotherapy has recently been verified to be an successful and promising cancer therapeutic strategy by us and numerous other studies. The obvious advantages of adenovirus as oncolytic virus vector include easy expansion and purification, suitable packaging capacity, good safety, and the ability to infect dividing and non-dividing cells et al, which made it as one of the most effective oncolytic virus candidate. However, there are some challenges about oncolytic adenovirus during clinical trials for cancer therapy. The most important concern is the neutralizing antibodies existed in the general population which may weaken oncolytic effect due to premature virus clearance. Therefore, many strategies have been developed to evade immune clearance of virus, which includes Ad fiber modifications, encapsulation using polymers, lipids and hydrogels, and use of MSC cells as virus carriers. Moreover, the low CAR expression in tumor cells also impeded adenovirus infection and replication, and hampered overall oncolytic efficacy. It was reported that Ad serotype 35 specifically infects target cells using CD46 as receptor. Thus, replacement of adenovirus 5 fiber with adenovirus 35 fiber can circumvent the low expression of CAR receptor in tumor cells, resulting in enhanced tumor-killing effect.

In conclusion, the Ad-GD55- α -TIM-3 vector was herein constructed as a novel oncolytic adenoviral vector encoding monoclonal anti-TIM-3. This virus can readily inhibit HCC cell growth *in vitro* and *in vivo*, activating antitumor immune responses following intratumoral injection in xenograft model mice via modulating the composition of the TIME. As such, this novel Ad-GD55- α -TIM-3 adenovirus may represent an ideal candidate tool for the future management of HCC.

Declarations

Funding

The research leading to these results received funding from the Applied Research and Cultivation Program of Jiangxi Province, No. 20212BAG70043; the Public Welfare Technology Project of Zhejiang Province, No. LGF21H160033; Zhejiang Medical Technology Plan Project, No. 2021KY047; Hangzhou Science and Technology Bureau, No. 20201203B44; Hangzhou Medical Health Science and Technology Project, No. B20220173; the National Natural Science Foundation of China, No. 81803069 and the Grant for 521 talent project of ZSTU.

Conflicts of interest

All authors certify that they have no affiliations with or involvement in any organization or entity with any financial interest or non-financial interest in the subject matter or materials discussed in this manuscript.

Data availability statements

The authors confirm that the data supporting the findings of this study are available within the article and its supplementary materials.

Author Contribution

The writing part of the article was mainly completed by L.Q. and W.Y.G., the experimental part was mainly completed by L.Q. , and the technical support was provided by Z.L.L. , Z.H.L. , W.F. , W.H. , W.Y.Q. and W.X.Y. . All authors reviewed the manuscript.

References

1. Bailly, C., Thuru, X., Goossens, L., and Goossens, J. F. (2023). Soluble TIM-3 as a biomarker of progression and therapeutic response in cancers and other of human diseases. *Biochemical pharmacology* 209: 115445.
2. Cao, W., Li, M., Liu, J., Zhang, S., Noordam, L., Verstegen, M. M. A., Wang, L., Ma, B., Li, S., Wang, W., Bolkestein, M., Doukas, M., Chen, K., Ma, Z., Bruno, M., Sprengers, D., Kwekkeboom, J., van der Laan, L. J. W., Smits, R., Peppelenbosch, M. P., and Pan, Q. (2020). LGR5 marks targetable tumor-initiating cells in mouse liver cancer. *Nature communications* 11: 1961.
3. Chen, K., Ma, J., Jia, X., Ai, W., Ma, Z., and Pan, Q. (2019). Advancing the understanding of NAFLD to hepatocellular carcinoma development: From experimental models to humans. *Biochimica et biophysica acta Reviews on cancer* 1871: 117-125.
4. Chen, L., Hong, J., Hu, R., Yu, X., Chen, X., Zheng, S., Qin, Y., Zhou, X., Wang, Y., Zheng, L., Fang, H., Liu, P., and Huang, B. (2021). Clinical Value of Combined Detection of Serum sTim-3 and Pepsinogen for Gastric Cancer Diagnosis. *Cancer management and research* 13: 7759-7769.
5. Chen, L., Qin, Y., Lin, B., Yu, X., Zheng, S., Zhou, X., Liu, X., Wang, Y., Huang, B., Jin, J., and Wang, L. (2022a). Clinical value of the sTim-3 level in chronic kidney disease. *Experimental and therapeutic medicine* 24: 606.
6. Chen, L., Yu, X., Lv, C., Dai, Y., Wang, T., Zheng, S., Qin, Y., Zhou, X., Wang, Y., Pei, H., Fang, H., and Huang, B. (2022b). Increase in Serum Soluble Tim-3 Level Is Related to the Progression of Diseases After Hepatitis Virus Infection. *Frontiers in medicine* 9: 880909.
7. Chesney, J., Puzanov, I., Collichio, F., Singh, P., Milhem, M. M., Glaspy, J., Hamid, O., Ross, M., Friedlander, P., Garbe, C., Logan, T. F., Hauschild, A., Lebbé, C., Chen, L., Kim, J. J., Gansert, J., Andtbacka, R. H. I., and Kaufman, H. L. (2018). Randomized, Open-Label Phase II Study Evaluating the Efficacy and Safety of Talimogene Laherparepvec in Combination With Ipilimumab Versus

- Ipilimumab Alone in Patients With Advanced, Unresectable Melanoma. *Journal of clinical oncology : official journal of the American Society of Clinical Oncology* 36: 1658-1667.
8. Cox, A. G., Hwang, K. L., Brown, K. K., Evason, K., Beltz, S., Tsomides, A., O'Connor, K., Galli, G. G., Yimlamai, D., Chhangawala, S., Yuan, M., Lien, E. C., Wucherpfennig, J., Nissim, S., Minami, A., Cohen, D. E., Camargo, F. D., Asara, J. M., Houvras, Y., Stainier, D. Y. R., and Goessling, W. (2016). Yap reprograms glutamine metabolism to increase nucleotide biosynthesis and enable liver growth. *Nature cell biology* 18: 886-896.
 9. Czauderna, C., Castven, D., Mahn, F. L., and Marquardt, J. U. (2019). Context-Dependent Role of NF- κ B Signaling in Primary Liver Cancer-from Tumor Development to Therapeutic Implications. *Cancers* 11.
 10. Das, R., Langou, S., Le, T. T., Prasad, P., Lin, F., and Nguyen, T. D. (2021). Electrical Stimulation for Immune Modulation in Cancer Treatments. *Frontiers in bioengineering and biotechnology* 9: 795300.
 11. Huang, H., Liu, Y., Liao, W., Cao, Y., Liu, Q., Guo, Y., Lu, Y., and Xie, Z. (2019). Oncolytic adenovirus programmed by synthetic gene circuit for cancer immunotherapy. *Nature communications* 10: 4801.
 12. Hwang, J. K., Hong, J., and Yun, C. O. (2020). Oncolytic Viruses and Immune Checkpoint Inhibitors: Preclinical Developments to Clinical Trials. *International journal of molecular sciences* 21.
 13. Ishino, R., Kawase, Y., Kitawaki, T., Sugimoto, N., Oku, M., Uchida, S., Imataki, O., Matsuoka, A., Taoka, T., Kawakami, K., van Kuppevelt, T. H., Todo, T., Takaori-Kondo, A., and Kadowaki, N. (2021). Oncolytic Virus Therapy with HSV-1 for Hematological Malignancies. *Molecular therapy : the journal of the American Society of Gene Therapy* 29: 762-774.
 14. Jia, X., Liu, Y., Cheng, Y., Wang, Y., Kang, H., Ma, Z., and Chen, K. (2022). Inosine monophosphate dehydrogenase type1 sustains tumor growth in hepatocellular carcinoma. *Journal of clinical laboratory analysis* 36: e24416.
 15. Ju, F., Luo, Y., Lin, C., Jia, X., Xu, Z., Tian, R., Lin, Y., Zhao, M., Chang, Y., Huang, X., Li, S., Ren, W., Qin, Y., Yu, M., Jia, J., Han, J., Luo, W., Zhang, J., Fu, G., Ye, X., Huang, C., and Xia, N. (2022). Oncolytic virus expressing PD-1 inhibitors activates a collaborative intratumoral immune response to control tumor and synergizes with CTLA-4 or TIM-3 blockade. *Journal for immunotherapy of cancer* 10.
 16. Kim, H., Kim, H., Feng, Y., Li, Y., Tamiya, H., Tocci, S., and Ronai, Z. A. (2020). PRMT5 control of cGAS/STING and NLRC5 pathways defines melanoma response to antitumor immunity. *Science translational medicine* 12.
 17. Lang, F. F., Conrad, C., Gomez-Manzano, C., Yung, W. K. A., Sawaya, R., Weinberg, J. S., Prabhu, S. S., Rao, G., Fuller, G. N., Aldape, K. D., Gumin, J., Vence, L. M., Wistuba, I., Rodriguez-Canales, J., Villalobos, P. A., Dirven, C. M. F., Tejada, S., Valle, R. D., Alonso, M. M., Ewald, B., Peterkin, J. J., Tufaro, F., and Fueyo, J. (2018). Phase I Study of DNX-2401 (Delta-24-RGD) Oncolytic Adenovirus: Replication and Immunotherapeutic Effects in Recurrent Malignant Glioma. *Journal of clinical oncology : official journal of the American Society of Clinical Oncology* 36: 1419-1427.
 18. LaRocca, C. J., and Warner, S. G. (2018). Oncolytic viruses and checkpoint inhibitors: combination therapy in clinical trials. *Clinical and translational medicine* 7: 35.

19. Lebbé, C., Meyer, N., Mortier, L., Marquez-Rodas, I., Robert, C., Rutkowski, P., Menzies, A. M., Eigentler, T., Ascierto, P. A., Smylie, M., Schadendorf, D., Ajaz, M., Svane, I. M., Gonzalez, R., Rollin, L., Lord-Bessen, J., Saci, A., Grigoryeva, E., and Pigozzo, J. (2019). Evaluation of Two Dosing Regimens for Nivolumab in Combination With Ipilimumab in Patients With Advanced Melanoma: Results From the Phase IIIb/IV CheckMate 511 Trial. *Journal of clinical oncology : official journal of the American Society of Clinical Oncology* 37: 867-875.
20. Li, H., Wu, K., Tao, K., Chen, L., Zheng, Q., Lu, X., Liu, J., Shi, L., Liu, C., Wang, G., and Zou, W. (2012). Tim-3/galectin-9 signaling pathway mediates T-cell dysfunction and predicts poor prognosis in patients with hepatitis B virus-associated hepatocellular carcinoma. *Hepatology (Baltimore, Md)* 56: 1342-1351.
21. Li, Q., Chen, Q., Klauser, P. C., Li, M., Zheng, F., Wang, N., Li, X., Zhang, Q., Fu, X., Wang, Q., Xu, Y., and Wang, L. (2020). Developing Covalent Protein Drugs via Proximity-Enabled Reactive Therapeutics. *Cell* 182: 85-97.e16.
22. Li, Z., Li, N., Li, F., Zhou, Z., Sang, J., Chen, Y., Han, Q., Lv, Y., and Liu, Z. (2016). Immune checkpoint proteins PD-1 and TIM-3 are both highly expressed in liver tissues and correlate with their gene polymorphisms in patients with HBV-related hepatocellular carcinoma. *Medicine* 95: e5749.
23. Lin, C. Z., Xiang, G. L., Zhu, X. H., Xiu, L. L., Sun, J. X., and Zhang, X. Y. (2018). Advances in the mechanisms of action of cancer-targeting oncolytic viruses. *Oncology letters* 15: 4053-4060.
24. Minott, J. A., van Vloten, J. P., Chan, L., Mehrani, Y., Bridle, B. W., and Karimi, K. (2022). The Role of Neutrophils in Oncolytic Orf Virus-Mediated Cancer Immunotherapy. *Cells* 11.
25. Monney, L., Sabatos, C. A., Gaglia, J. L., Ryu, A., Waldner, H., Chernova, T., Manning, S., Greenfield, E. A., Coyle, A. J., Sobel, R. A., Freeman, G. J., and Kuchroo, V. K. (2002). Th1-specific cell surface protein Tim-3 regulates macrophage activation and severity of an autoimmune disease. *Nature* 415: 536-541.
26. Qin, S., Dong, B., Yi, M., Chu, Q., and Wu, K. (2020). Prognostic Values of TIM-3 Expression in Patients With Solid Tumors: A Meta-Analysis and Database Evaluation. *Frontiers in oncology* 10: 1288.
27. Raja, J., Ludwig, J. M., Gettinger, S. N., Schalper, K. A., and Kim, H. S. (2018). Oncolytic virus immunotherapy: future prospects for oncology. *Journal for immunotherapy of cancer* 6: 140.
28. Ribas, A., Dummer, R., Puzanov, I., VanderWalde, A., Andtbacka, R. H. I., Michielin, O., Olszanski, A. J., Malvehy, J., Cebon, J., Fernandez, E., Kirkwood, J. M., Gajewski, T. F., Chen, L., Gorski, K. S., Anderson, A. A., Diede, S. J., Lassman, M. E., Gansert, J., Hodi, F. S., and Long, G. V. (2017). Oncolytic Virotherapy Promotes Intratumoral T Cell Infiltration and Improves Anti-PD-1 Immunotherapy. *Cell* 170: 1109-1119.e1110.
29. Sabatos-Peyton, C. A., Nevin, J., Brock, A., Venable, J. D., Tan, D. J., Kassam, N., Xu, F., Taraszka, J., Wesemann, L., Pertel, T., Acharya, N., Klapholz, M., Etminan, Y., Jiang, X., Huang, Y. H., Blumberg, R. S., Kuchroo, V. K., and Anderson, A. C. (2018). Blockade of Tim-3 binding to phosphatidylserine and CEACAM1 is a shared feature of anti-Tim-3 antibodies that have functional efficacy. *Oncoimmunology* 7: e1385690.

30. Samson, A., West, E. J., Carmichael, J., Scott, K. J., Turnbull, S., Kuszlewicz, B., Dave, R. V., Peckham-Cooper, A., Tidswell, E., Kingston, J., Johnpulle, M., da Silva, B., Jennings, V. A., Bendjama, K., Stojkowitz, N., Lusky, M., Prasad, K. R., Toogood, G. J., Auer, R., Bell, J., Twelves, C. J., Harrington, K. J., Vile, R. G., Pandha, H., Errington-Mais, F., Ralph, C., Newton, D. J., Anthoney, A., Melcher, A. A., and Collinson, F. (2022). Neoadjuvant Intravenous Oncolytic Vaccinia Virus Therapy Promotes Anticancer Immunity in Patients. *Cancer immunology research* 10: 745-756.
31. Sung, H., Ferlay, J., Siegel, R. L., Laversanne, M., Soerjomataram, I., Jemal, A., and Bray, F. (2021). Global Cancer Statistics 2020: GLOBOCAN Estimates of Incidence and Mortality Worldwide for 36 Cancers in 185 Countries. *CA: a cancer journal for clinicians* 71: 209-249.
32. Tang, W., Chen, Z., Zhang, W., Cheng, Y., Zhang, B., Wu, F., Wang, Q., Wang, S., Rong, D., Reiter, F. P., De Toni, E. N., and Wang, X. (2020). The mechanisms of sorafenib resistance in hepatocellular carcinoma: theoretical basis and therapeutic aspects. *Signal transduction and targeted therapy* 5: 87.
33. Tang, Y., Li, K., Hu, B., Cai, Z., Li, J., Tao, H., and Cao, J. (2022). Fatty acid binding protein 5 promotes the proliferation, migration, and invasion of hepatocellular carcinoma cells by degradation of Krüppel-like factor 9 mediated by miR-889-5p via cAMP-response element binding protein. *Cancer biology & therapy* 23: 424-438.
34. Thongsri, P., Pewkliang, Y., Borwornpinyo, S., Wongkajornsilp, A., Hongeng, S., and Sa-Ngiamsumton, K. (2021). Curcumin inhibited hepatitis B viral entry through NTCP binding. *Scientific reports* 11: 19125.
35. Tseng, H. C., Xiong, W., Badeti, S., Yang, Y., Ma, M., Liu, T., Ramos, C. A., Dotti, G., Fritzky, L., Jiang, J. G., Yi, Q., Guarrera, J., Zong, W. X., Liu, C., and Liu, D. (2020). Efficacy of anti-CD147 chimeric antigen receptors targeting hepatocellular carcinoma. *Nature communications* 11: 4810.
36. Villanueva, A. (2019). Hepatocellular Carcinoma. *The New England journal of medicine* 380: 1450-1462.
37. Wang, G., Kang, X., Chen, K. S., Jehng, T., Jones, L., Chen, J., Huang, X. F., and Chen, S. Y. (2020). An engineered oncolytic virus expressing PD-L1 inhibitors activates tumor neoantigen-specific T cell responses. *Nature communications* 11: 1395.
38. Xiao, Y., Qing, J., Li, B., Chen, L., Nong, S., Yang, W., Tang, X., and Chen, Z. (2020). TIM-3 Participates in the Invasion and Metastasis of Nasopharyngeal Carcinoma via SMAD7/SMAD2/SNAIL1 Axis-Mediated Epithelial-Mesenchymal Transition. *OncoTargets and therapy* 13: 1993-2006.
39. Yang, Z. Y., Liu, L., Mao, C., Wu, X. Y., Huang, Y. F., Hu, X. F., and Tang, J. L. (2014). Chemotherapy with cetuximab versus chemotherapy alone for chemotherapy-naive advanced non-small cell lung cancer. *The Cochrane database of systematic reviews*: Cd009948.
40. Yi, M., Jiao, D., Xu, H., Liu, Q., Zhao, W., Han, X., and Wu, K. (2018). Biomarkers for predicting efficacy of PD-1/PD-L1 inhibitors. *Molecular cancer* 17: 129.
41. Ying, C., Xiao, B. D., Qin, Y., Wang, B. R., Liu, X. Y., Wang, R. W., Fang, L., Yan, H., Zhou, X. M., and Wang, Y. G. (2018). GOLPH2-regulated oncolytic adenovirus, GD55, exerts strong killing effect on

- human prostate cancer stem-like cells in vitro and in vivo. *Acta pharmacologica Sinica* 39: 405-414.
42. Yoshida, H., Sato-Dahlman, M., Hajeri, P., Jacobsen, K., Koodie, L., Yanagiba, C., Shanley, R., and Yamamoto, M. (2021). Mutant myogenin promoter-controlled oncolytic adenovirus selectively kills PAX3-FOXO1-positive rhabdomyosarcoma cells. *Translational oncology* 14: 100997.
43. Zhang, Z. L., Zou, W. G., Luo, C. X., Li, B. H., Wang, J. H., Sun, L. Y., Qian, Q. J., and Liu, X. Y. (2003). An armed oncolytic adenovirus system, ZD55-gene, demonstrating potent antitumoral efficacy. *Cell research* 13: 481-489.
44. Zhu, C., Sakuishi, K., Xiao, S., Sun, Z., Zaghouani, S., Gu, G., Wang, C., Tan, D. J., Wu, C., Rangachari, M., Pertel, T., Jin, H. T., Ahmed, R., Anderson, A. C., and Kuchroo, V. K. (2015). An IL-27/NFIL3 signalling axis drives Tim-3 and IL-10 expression and T-cell dysfunction. *Nature communications* 6: 6072.

Figures

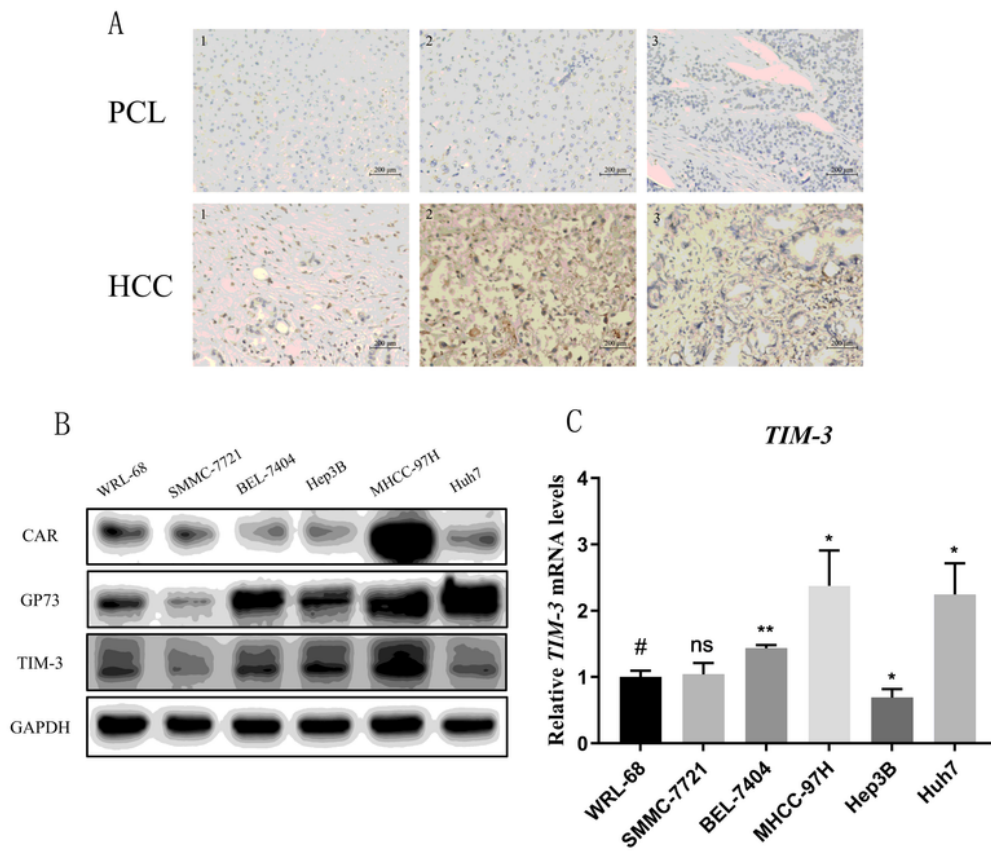


Figure 1

Analyses of TIM-3 expression in tumors and HCC cells. A. TIM-3 levels in liver cancer patients were detected via immunohistochemistry. B. Western blotting was used to assess CAR, GP73, and TIM-3 levels in HCC cells. C. TIM-3 mRNA levels were analyzed via qPCR. Data are means \pm SD. n=3. **P<0.01; ***P<0.001. NS, not significant.

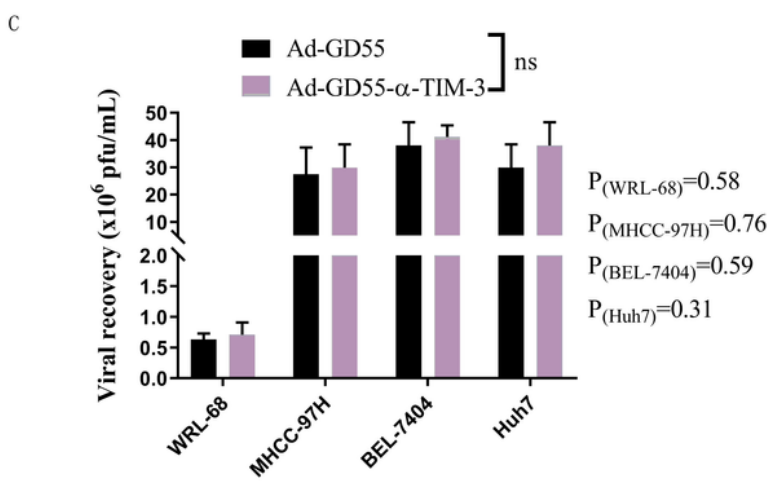
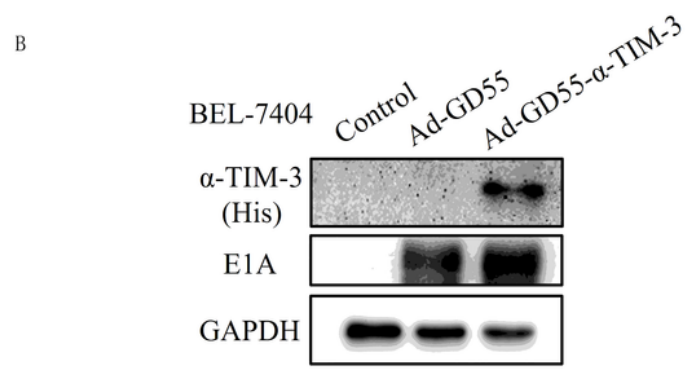
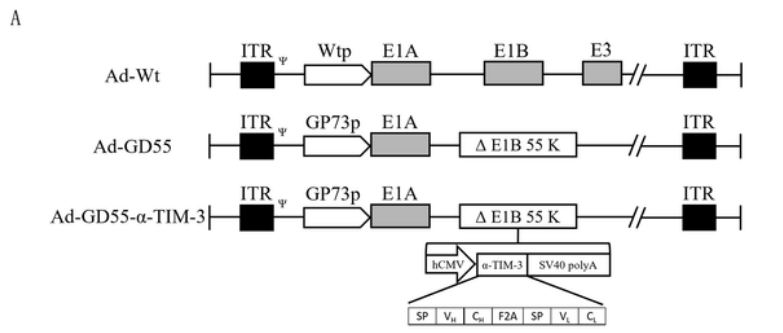
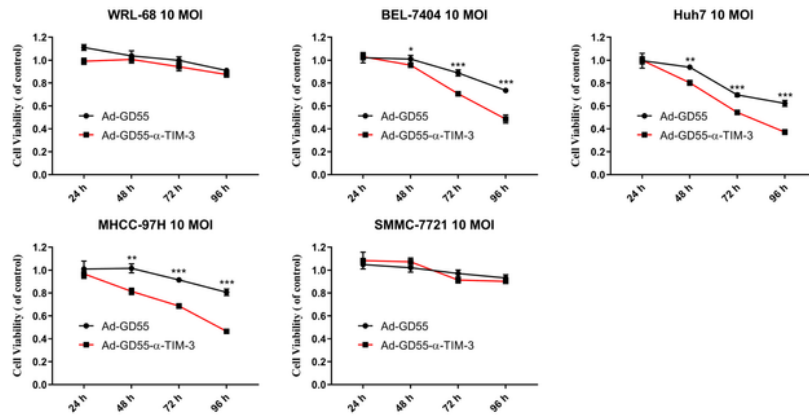


Figure 2

Ad-GD55-α-TIM-3 construction and overview. A. A schematic overview of the structure of the constructed oncolytic virus. B. α-TIM-3 and viral E1A levels induced by Ad-GD55 were detected by Western immunoblotting. C. Viral progeny assay. WRL-68, Huh7, BEL-7404, and MHCC-97H cells were infected with Ad-GD55 or Ad-GD55-α-TIM-3 (MOI = 10). A TCID₅₀ assay was used to detect viral titer.

A



B

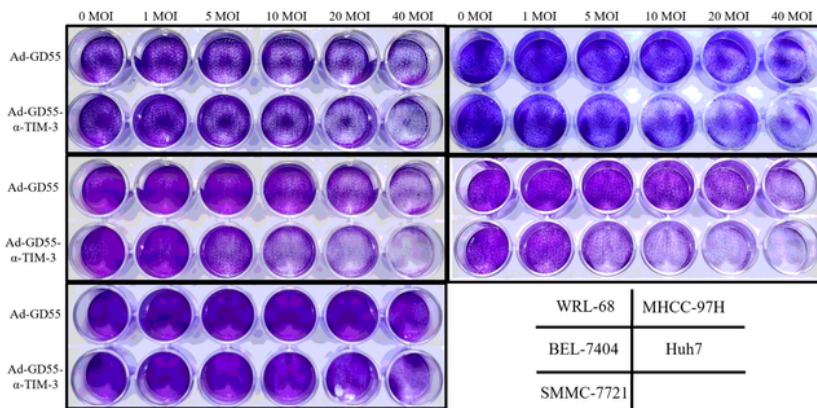


Figure 3

Ad-GD55-α-TIM-3 inhibits *in vitro* HCC cell viability. A. WRL-68, Huh7, BEL-7404, and MHCC-97H cells were infected with Ad-GD55 or Ad-GD55-α-TIM-3 (MOI = 10) for a range of time intervals, and an MTT assay was used to quantify cellular viability. Data are means ± SD. n=3. *P<0.05; ***P<0.001. B. These cell lines were infected with Ad-GD55 or Ad-GD55-α-TIM-3 at various MOIs (0, 1, 5, 10, 20, 40 MOIs), followed by

crystal violet staining three days later to assess the cytopathic effect, with representative images being shown.

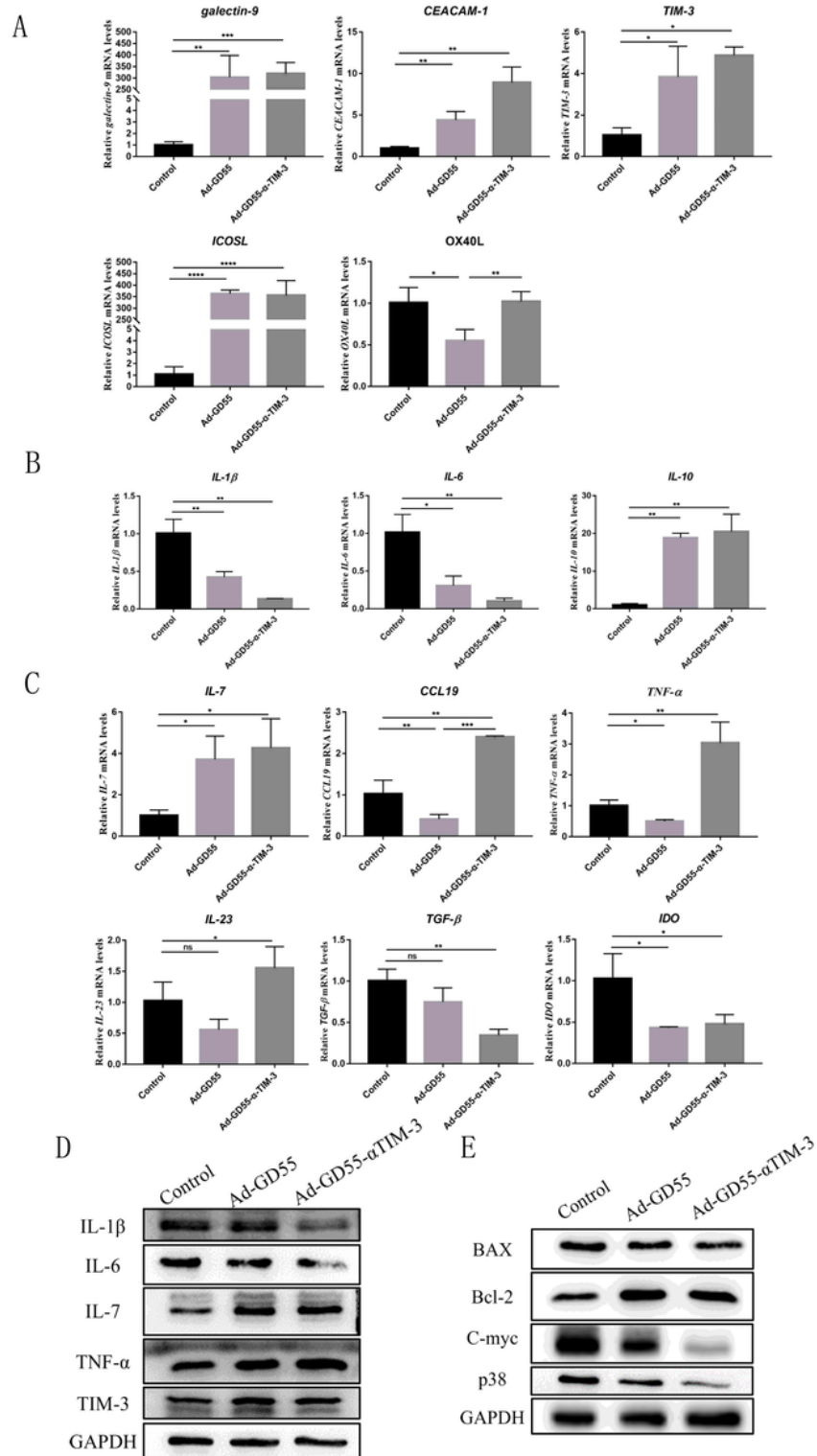


Figure 4

Evaluation of the mechanistic basis for the antitumor efficacy of Ad-GD55- α -TIM-3. A. qPCR was used to detect IL-1 β , IL-5, and IL-10 expression in Bel-7404 cells following a 48 h infection with Ad-GD55- α -TIM-3

(MOI = 10). B. Cells were treated as in A and qPCR was used to detect co-inhibitor and co-stimulatory genes (galectin-9, CEACAM-1, TIM-3, ICOSL, OX40L). C. Cells were treated as in A and qPCR was used to detect immune-related genes including IL-7, CCL19, TNF- α , IL-23 TGF- β , and IDO. D, E. Western immunoblotting was used to detect (D) immune-related factors and (E) growth and apoptosis-related proteins. Data are means \pm SD. n=3. **P<0.01; ***P<0.001. NS, not significant.

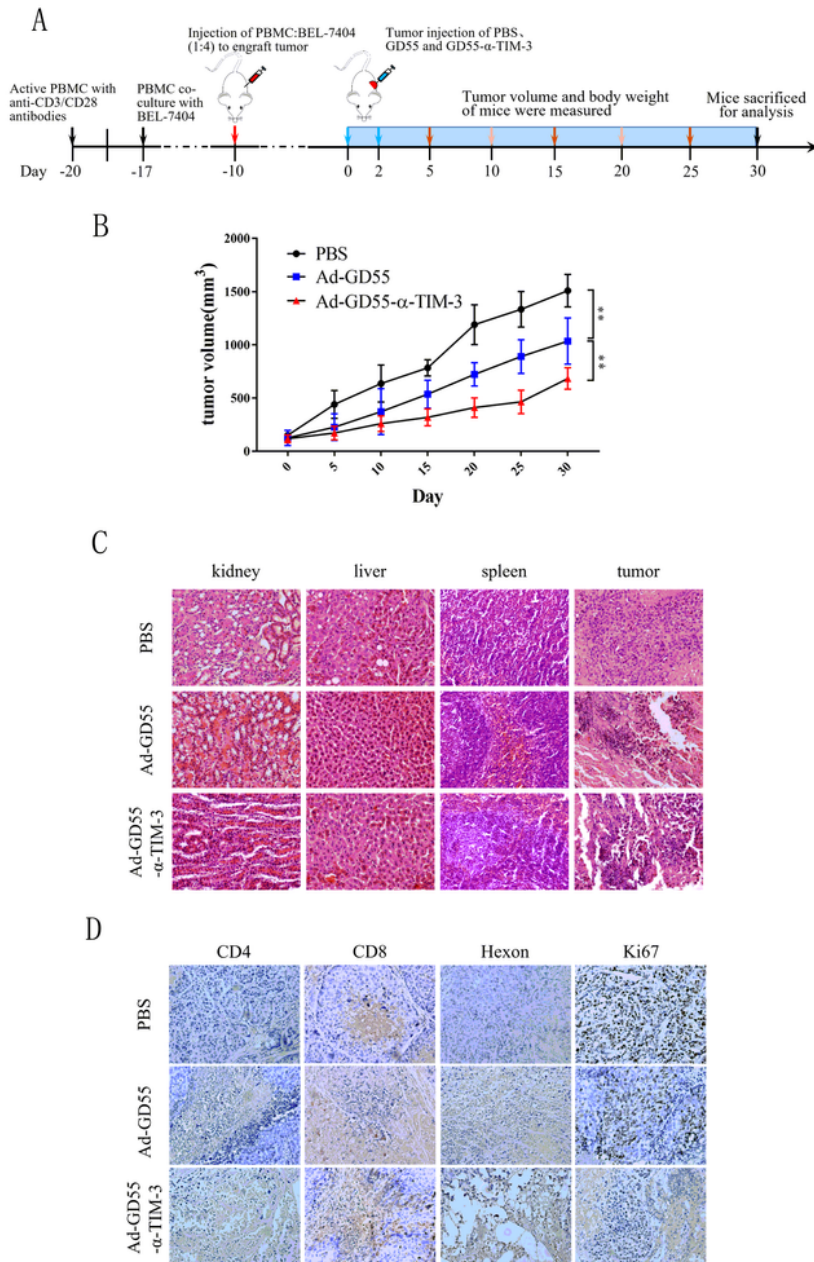


Figure 5

In vivo analyses of the antitumor efficacy of Ad-GD55- α -TIM-3. A. Schematic overview of the animal study approach. Following the activation of PBMCs with anti-CD3/CD28, cells were cultured together with BEL-7404 cells at a 1:4 ratio (BEL-7404 = 1×10^7 , PBMC = 2.5×10^6). Female nude BALB/c mice (6-8 weeks old) were subcutaneously injected with these mixed cells. When tumors were $\sim 100 \text{ mm}^3$, mice were intratumorally injected with PBS, Ad-GD55 (1×10^9 PFU/100 μL), and Ad-GD55- α -TIM-3 (1×10^9 PFU/100 μL) every other day for two total injections. B. Tumor volume was measured every 5 days in the indicated groups following viral treatment with the following formula: $V = (\text{length} \times \text{width}^2) / 2$. C. Histopathological effect was detected by HE staining. D. The expression of adenoviral hexon, CD4, CD8, and Ki-67 were detected via immunohistochemistry.

Supplementary Files

This is a list of supplementary files associated with this preprint. Click to download.

- [SupplementalMaterials.docx](#)